Legends for supplementary figures

Supplementary Fig. 1. Bioinformatics analyses of *T. gondii* AKMT. (**a**) Folding predictions of full-length *T. gondii* AKMT obtained using the FoldIndex algorithm [1] suggested that its N-terminal ~300 amino acids are completely disordered and the rest of the protein is mostly folded. (**b**) Domain arrangement of AKMT and primary sequence alignment of AKMT with orthologs from various apicomplexan species and their free-living relatives (*Chromera* and *Vitrolla*) in the superphylum of Alveolata, together with mammalian SMYD1-3. Domains and domain boundaries in AKMT are indicated above the aligned sequences. The MYND domains in SYMD1-3 are indicated by a red box. The alignments were carried using the option of "Mafft with defaults" in Jalview, with residues highlighted using the Clustal color scheme.

Supplementary Fig. 2. Secondary structure assignments of the AKMT crystal structure. The secondary structures were calculated using PDBsum [2], with all α-helices and β-strands sequentially numbered.

Supplementary Fig. 3. Methylated lysine residues in the crystal structure. (**a**) Table listing all lysine residues of the four AKMT molecules in the asymmetric unit. Unmodified, mono-methyl, and di-methyl lysines are highlighted in blue, magenta, and green colors, respectively. Marked with asterisks are the mono-methyl lysines adopting two different conformations in the structure. Arrows mark the representative residues shown in (b). (**b**) 2Fo-Fc maps (contoured at 1.0 σ) of the representative lysine residues that are well-resolved in the refined structure. The same residues in all four molecules of the asymmetric unit are shown side-by-side for direct comparisons. (**c**) 2Fo-Fc maps (contoured at 1.2 σ) for the representative small molecules of each type present in the refined model, including one glycerol (GOL), one di(hydroxyethyl)ether (PEG), and three ethylene glycols (EDO).

Supplementary Fig. 4. Intermolecular contacts between neighboring molecules in the asymmetric unit of the crystal. Buried surface area (BSA), Gibbs free energy (ΔiG), and numbers of hydrogen bonds and salt bridges for each intermolecular contact site are shown around the structure. Details of the hydrogen bonds in each case are also listed. The analyses were carried out on the PDBePISA server [3].

Supplementary Fig. 5. Three independent ITC measurements for the interaction between an AKMT protein and cofactor SAM or SFG. Average molar ratios (N) and K_d values are listed at the bottom of each column.

Supplementary Fig. 6. Comparison of AKMT with SAM-bound SMYD2. (**a**) Superposition of AKMT chain A (rainbow color), together with the swapped N-terminus of neighboring chain C (magenta), on top of the SAM-bound SMYD2 structure (5ARG.pdb, gray). Note the overlap of the putative cofactor binding site with the residue K312 of AKMT, which is due to domain swap that causes the flip of the preceding β1 from the antiparallel position (i.e. chain C) to a fully extended conformation in chain A. (**b**) 2Fo-Fc map (contoured at 1.0 σ) around the hinge of the swapped region. Note the unusual *cis*-conformation of the residue G311, which allows residue K312 (di-methylated) to loop out into the putative cofactor binding pocket defined partly by residue Y481.

Supplementary Fig. 7. Other representative TPR-mediated homodimeric proteins. (**a**) The N-N mediated dimer of the TPR domains of the *S. pombe* APC/C subunit Cut9. (**b**) The C-C mediated dimer of the TPR domains of the light chain of mammalian kinesin-1. (**c**) The M-M dimeric arrangement of the superhelical TPR domains of human O-linked GlcNAc transferase.

Supplementary Fig. 8. Structural comparison of AKMT with SMYD3 analyzed by RAPIDO [4]. (**a**) Summary of structural alignments of AKMT with SMYD1-3 carried out by RAPIDO. The table shows values of rmsd and numbers of aligned residues, with each structure either as a single rigid body (rigid) or as multiple flexible rigid bodies (flex). (**b**) Details of the flexible alignment between AKMT and SMYD3 structures. Two local rigid bodies are identified by RAPIDO. Aligned structures based on the first (No. 1) and second (No. 2) rigid bodies are shown in (c-e) and (f-h), respectively. (**c and f**) Superposition of AKMT onto SMYD3 based on rigid body No. 1 (c) and No. 2 (f). (**d and g**) Extracted view of the aligned rigid bodies in (c, f). (**e and h**) Two orthogonal views of the ribbon diagrams of the aligned regions shown in (d, g).

Supplementary Fig. 9. SAXS analyses of the monomeric mutant of AKMT. (**a**) Overlay of the AKMT-ΔNTD monomeric structure (magenta cartoon) onto the *ab initio* low resolution

SAXS model of AKMT-ΔNTD-4A obtained in the standard batch mode measurement. (**b**) Fitting of the crystal structure of AKMT-ΔNTD monomer into the *ab initio* SAXS model of AKMT-ΔNTD-4A generated by the SEC-coupled SAXS measurement. The encircled "tail" in the *ab initio* model in (a) is likely caused by the transient interaction between two AKMT monomers; such extra densities are not present in the SEC-SAXS model in (b).

References:

1. Prilusky, J., et al., *FoldIndex: a simple tool to predict whether a given protein sequence is intrinsically unfolded*. Bioinformatics, 2005. **21**(16): p. 3435-8.
2. Laskowski, R.A., *Enhancing the functional annotation of PDB structures in PDBsum using key figures extracted from the literature.* Bioinformatics, 2007. **23**(14): p. 1824-7.
3. Krissinel, E. and K. Henrick, *Inference of macromolecular assemblies from crystalline state.* J Mol Biol, 2007. **372**(3): p. 774-97.
4. Mosca, R. and T.R. Schneider, *RAPIDO: a web server for the alignment of protein structures in the presence of conformational changes.* Nucleic Acids Res, 2008. **36**(Web Server issue): p. W42-6.

Supplementary Fig. 1

Supplementary Fig. 2

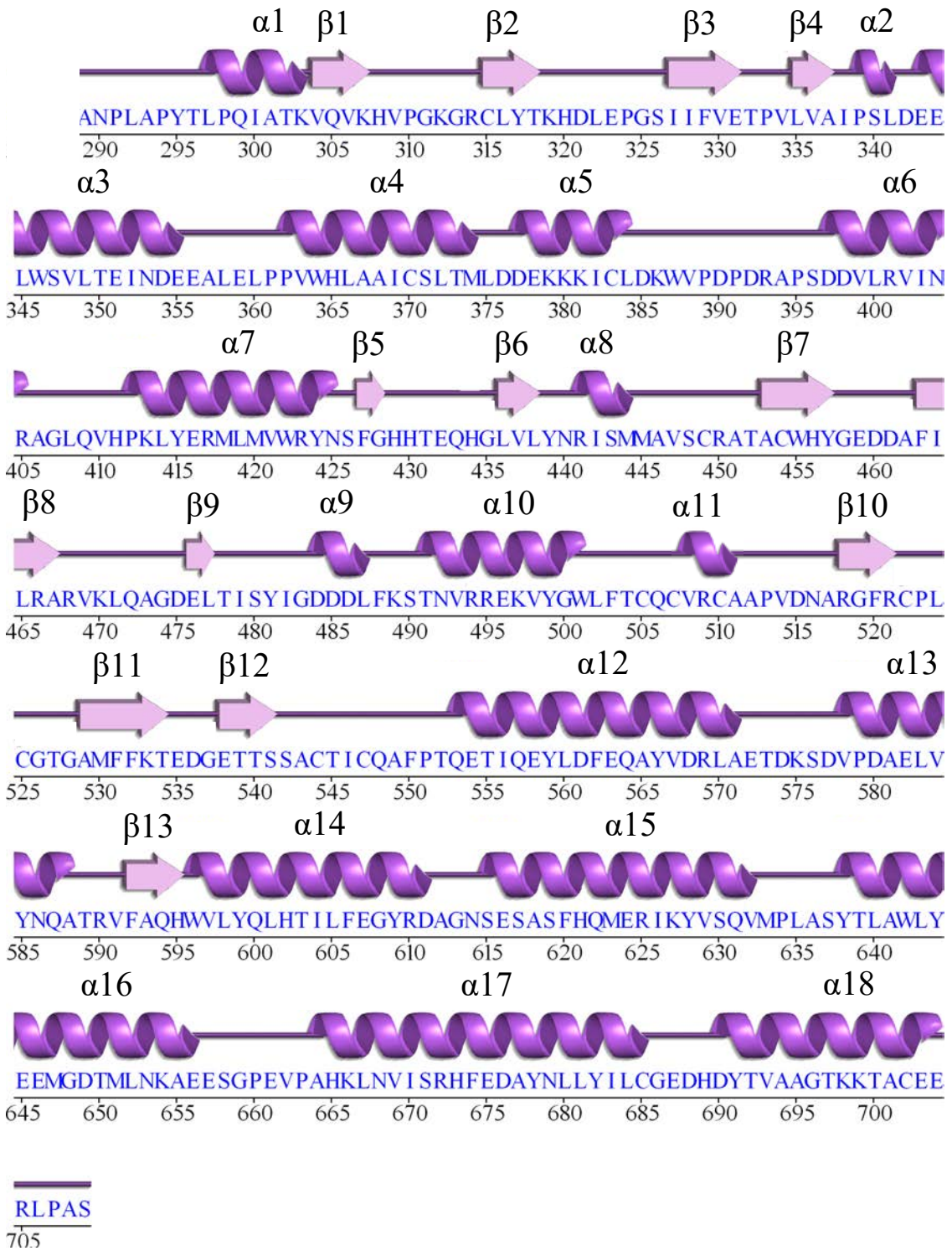

Supplementary Fig. 3

(a)

Residue # \ Chain ID	A	B	C	D
→ 303	MLY	MLZ	LYS	MLZ
307	MLY	MLY	LYS	MLY
→ 312	MLY	MLY	MLY	MLY
319	LYS	MLZ	MLY	MLY
379	LYS	MLZ*	LYS	MLY
380	MLZ	LYS	MLZ	MLZ
381	LYS	LYS	LYS	LYS
386	LYS	LYS	LYS	LYS
413	LYS	MLY	LYS	MLY
→ 470	MLZ	LYS	MLY	MLY
→ 489	MLY	MLY	MLY	MLY
497	MLY	MLZ	MLY	MLY
533	LYS	MLZ	LYS	MLZ
→ 575	LYS	MLZ	MLY	LYS
627	MLY	MLY	MLY	MLY
654	LYS	MLZ	LYS	LYS
666	MLY	MLZ	MLY	MLZ
→ 698	LYS	LYS	LYS	MLZ
→ 699	LYS	MLZ*	MLZ	LYS

LYS: lysine; **MLZ:** mono-methyl lysine; **MLY:** di-methyl lysine. * Two conformations

(b)

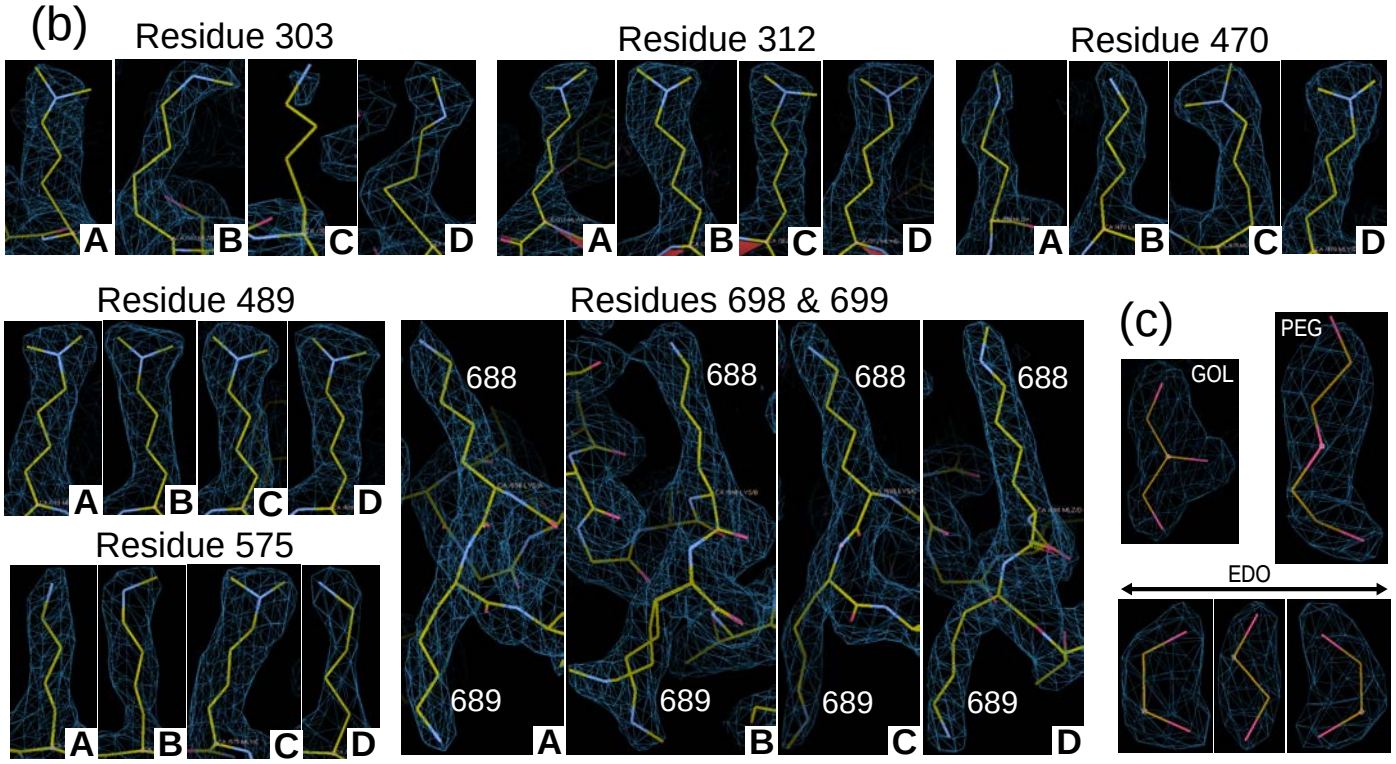

(c)

Supplementary Fig. 4

Hydrogen bonds

##	Chain A	Dist.[Å]	Chain B
1	R672[NH2]	3.34	G526[O]
2	N679[ND2]	2.95	T527[OG1]
3	K470[N]	2.84	C547[O]
4	R521[NH1]	3.28	D676[OD1]
5	T527[OG1]	2.81	D676[OD1]
6	G526[O]	3.29	R672[NH2]
7	T527[OG1]	3.18	N679[ND2]
8	C547[O]	2.89	K470[N]
9	D676[OD1]	2.93	T527[OG1]
10	D676[OD1]	3.19	R521[NH1]

Salt bridges

##	Chain A	Dist.[Å]	Chain B
1	R521[NH1]	3.28	D676[OD1]
2	D676[OD1]	3.19	R521[NH1]

Hydrogen bonds

##	Chain C	Dist.[Å]	Chain D
1	R672[NH2]	3.26	G526[O]
2	N679[ND2]	2.97	T527[OG1]
3	K470[N]	2.81	C547[O]
4	R521[NH1]	3.32	D676[OD1]
5	T527[OG1]	2.77	D676[OD1]
6	G526[O]	3.24	R672[NH2]
7	T527[OG1]	3.09	N679[ND2]
8	C547[O]	2.83	K470[N]
9	D676[OD1]	2.86	T527[OG1]
10	D676[OD1]	3.38	R521[NH1]

Salt bridges

##	Chain C	Dist.[Å]	Chain D
1	R521[NH1]	3.32	D676[OD1]
2	D676[OD1]	3.38	R521[NH1]

BSA: 1758 Å² (16 HB)
Δ^iG = -23.9 kcal/mol

BSA: 1903 Å² (10 HB, 2 SB)
Δ^iG = -24.7 kcal/mol

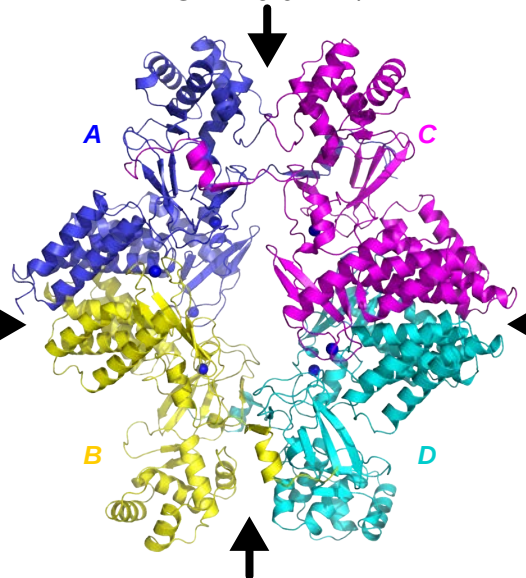

BSA: 1856 Å² (10 HB, 2 SB)
Δ^iG = -25.4 kcal/mol

BSA: buried surface area
HB: hydrogen bond
SB: salt bridge

BSA: 1835 Å² (15 HB)
Δ^iG = -25.0 kcal/mol

Hydrogen bonds

##	Chain A	Dist.[Å]	Chain C
1	Y295[N]	2.72	V330[O]
2	Y295[OH]	3.71	I328[O]
3	L297[O]	3.37	R441[NH1]
4	T302[O]	3.08	H320[NE2]
5	K303[O]	2.88	K319[N]
6	Q305[N]	2.66	Y317[O]
7	Q305[O]	2.90	Y317[N]
8	K307[N]	3.02	C315[O]
9	K307[O]	3.59	C315[N]
10	C315[N]	3.72	K307[O]
11	C315[O]	3.13	K307[N]
12	Y317[N]	3.26	Q305[O]
13	Y317[O]	2.69	Q305[N]
14	K319[N]	3.08	K303[O]
15	H320[NE2]	3.09	T302[O]
16	V330[O]	2.70	Y295[OH]

Hydrogen bonds

##	Chain B	Dist.[Å]	Chain D
1	Y295[N]	2.94	V330[O]
2	K303[O]	2.86	K319[N]
3	Q305[N]	2.72	Y317[O]
4	Q305[O]	3.00	Y317[N]
5	K307[N]	2.92	C315[O]
6	K307[O]	3.73	C315[N]
7	K307[O]	3.24	R314[NE]
8	C315[N]	3.66	K307[O]
9	C315[O]	3.00	K307[N]
10	Y317[N]	2.95	Q305[O]
11	Y317[O]	2.75	Q305[N]
12	K319[N]	2.79	K303[O]
13	K319[NZ]	2.98	A301[O]
14	H320[NE2]	3.37	T302[O]
15	V330[O]	2.85	Y295[N]

Supplementary Fig. 5

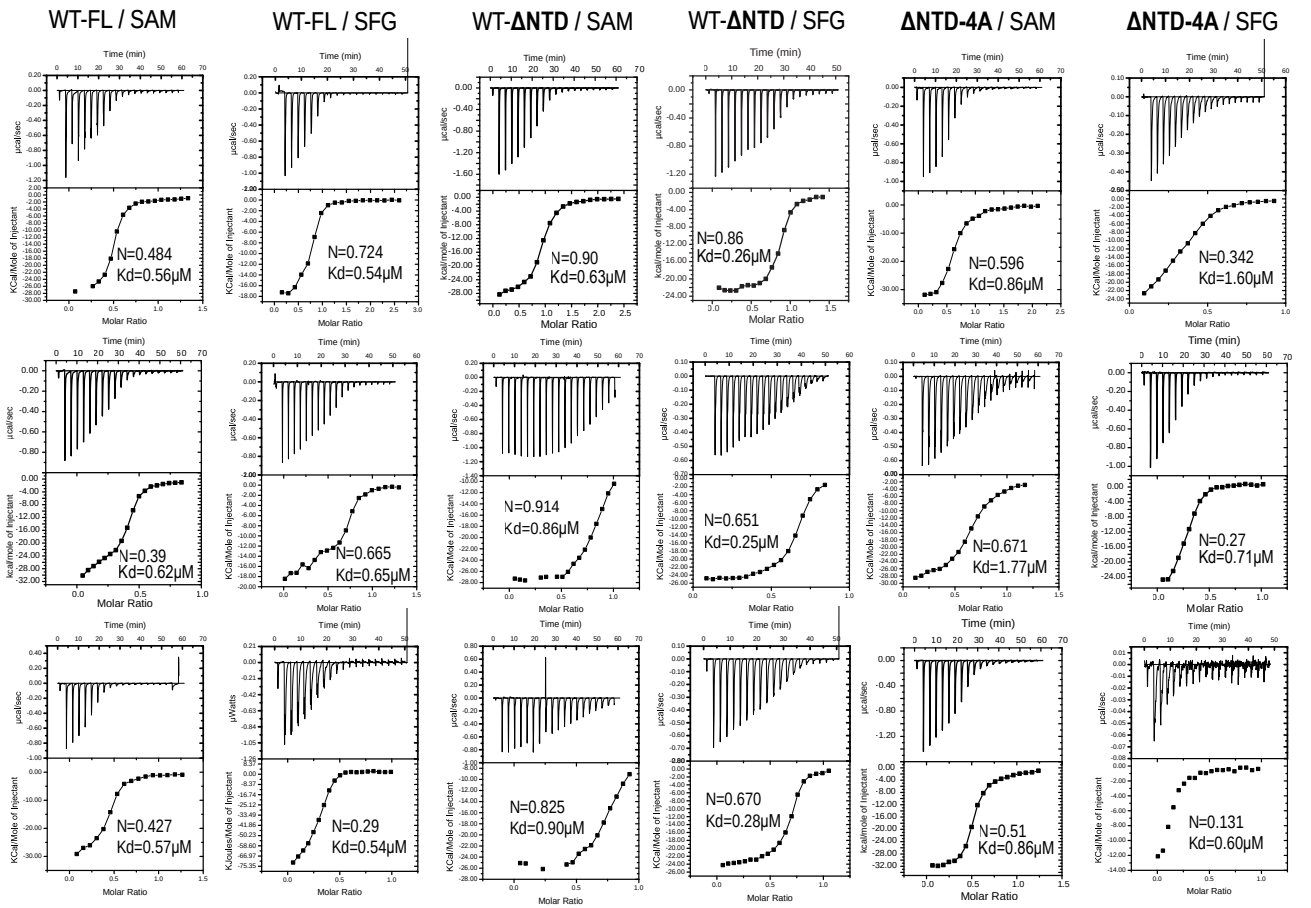

Average N=0.433±0.039
Average Kd=0.583±0.026μM

Average N=0.560±0.0192
Average Kd=0.576±0.052μM

Average N=0.880±0.039
Average Kd=0.797±0.119μM

Average N=0.727±0.094
Average Kd=0.263±0.012μM

Average N=0.592±0.066
Average Kd=1.163±0.429μM

Average N=0.248±0.088
Average Kd=0.970±0.448μM

Supplementary Fig. 6

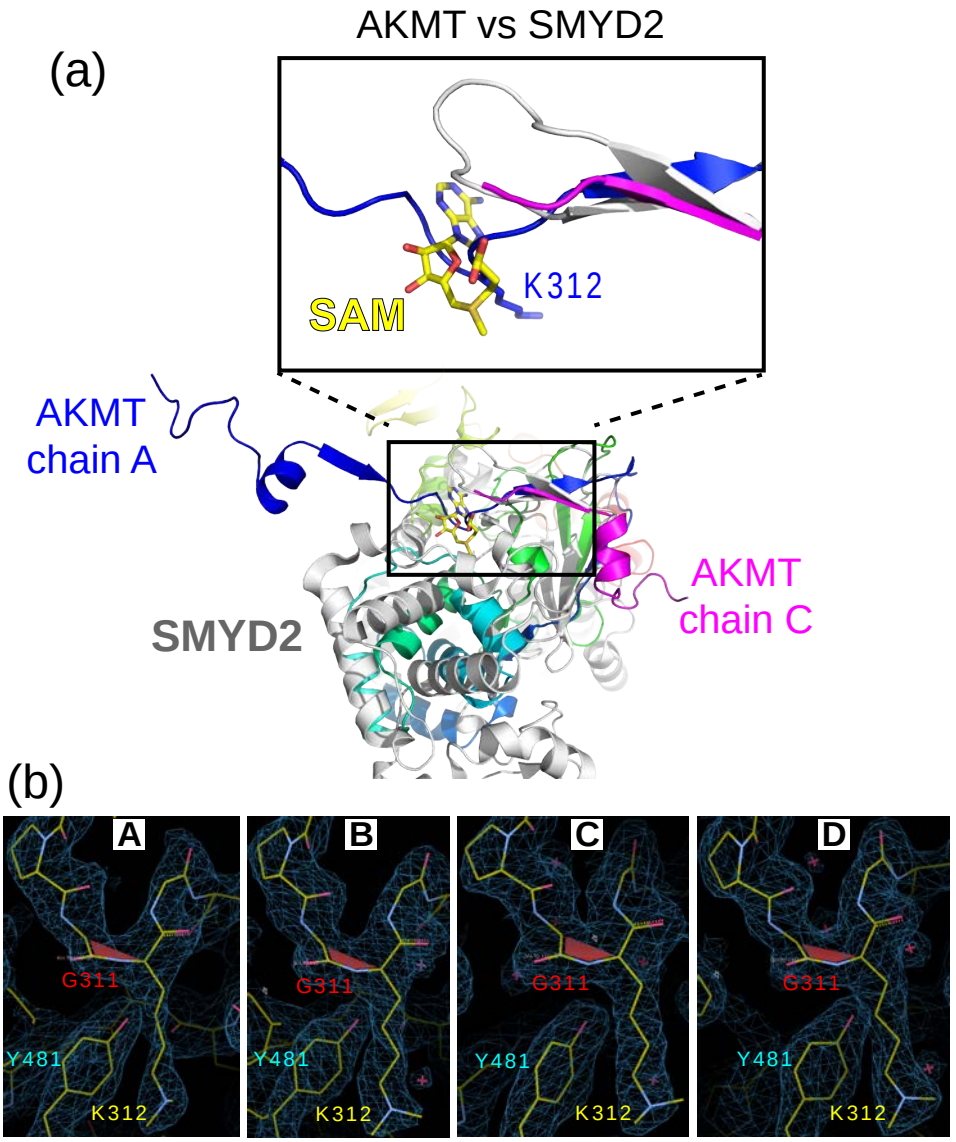

Supplementary Fig. 7

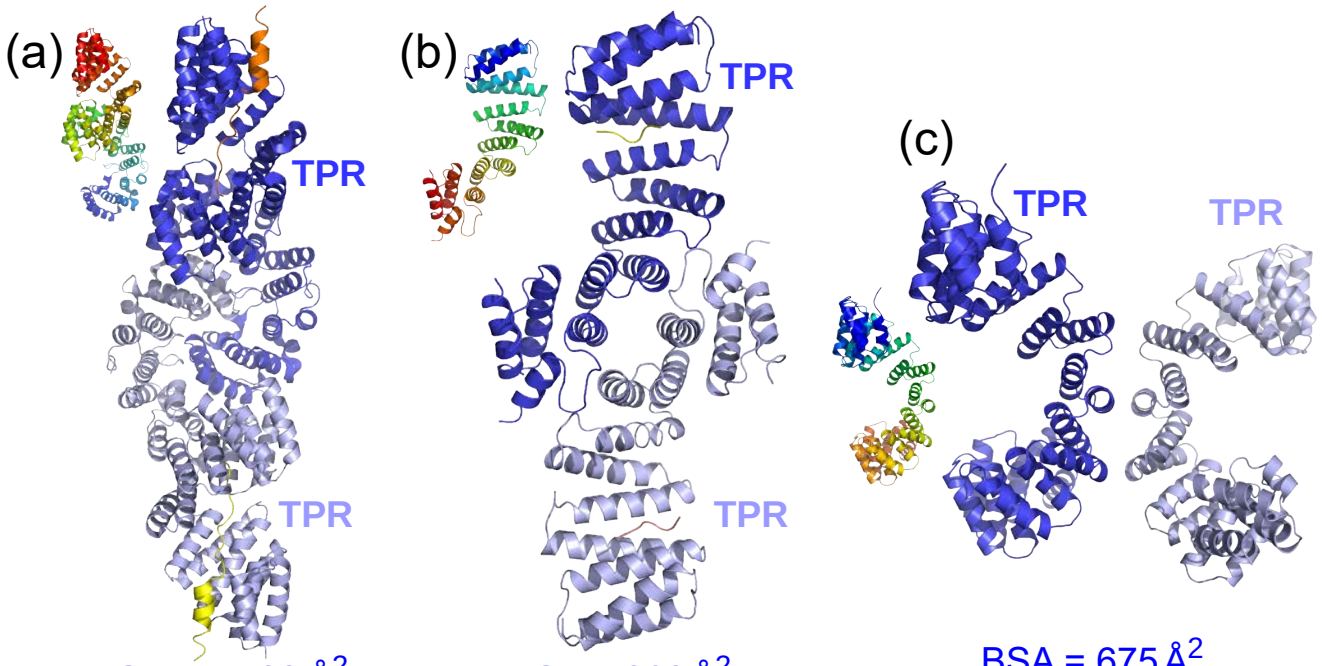

(a) **Statistics of structural alignments of AKMT with SMYD 1-3 by RAPIDO**

AKMT vs.	$RMSD_{rigid}$	#aa aligned	$RMSD_{flex}$ (Å)	# aa rigid	# rigid bodies
SMYD1 (3N71.pdb)	3.16	325	**1.34**	223	2
SMYD2 (5ARG.pdb)	3.90	317	**1.08**	228	2
SMYD3 (5EX0.pdb)	4.14	308	**1.20**	190	2

(b) **AKMT vs SMYD3 (rigid body-based structural alignments)**

Rigid bodies	# aa aligned	RMSD (Å)	Description	
No. 1	129	1.18	AKMT	A304-A307, A314-A336, A386-A388, A414-A427, A437-A457, A462-A482, A490-A510, A636-A637, A671-A672, A675-A687, A702-A706
			SMYD3 (5EX0.pdb)	A6-A9, A16-A38, A129-A131, A170-A183, A196-A216, A220-A240, A245-A254, A256-A266, A365-A366, A390-A391, A394-A406, A421-A425
No. 2	61	1.22	AKMT	A515-A520, A595-A630, A640-A652, A673-A674, A698-A701
			SMYD3 (5EX0.pdb)	A273-A278, A324-A359, A369-A381, A392-A393, A417-A420

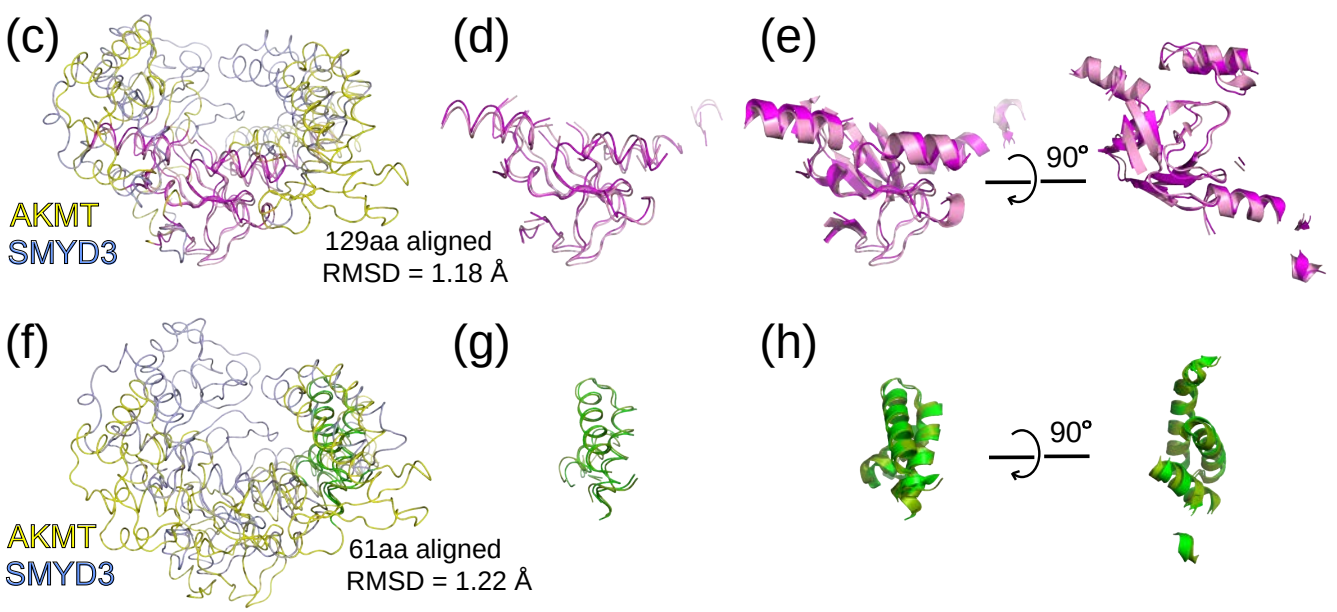

Supplementary Fig. 9